The Washing Effect of Fluid Motion on the Segregation of the Transitional Solidification Layers in Steel Ingots

By Tadayoshi TAKAHASHI,* Iwao HAGIWARA,** and Kiyoshi ICHIKAWA*

Synopsis

The effect of the fluid motion of bulk liquid on the effective distribution coefficient was studied in an Al–4 *wt%*Cu *alloy, using a special apparatus. The effective distribution coefficient is decreased with increasing the flow velocity of bulk liquid, because micro- and macro-segregation are controlled by the degree of washing against the region of partial solidification with the fluid flow of bulk liquid.*

I. Introduction

Fluid motion is caused by free convection, rimming action with evolution of CO gases and so on during the solidification of steel ingots, while the crystal growth of steel ingots shows dendrite morphology. Thus the relation between the fluid motion and dendrite morphology should not be neglected on the discussion of the segregation in steel ingots. In order to understand the phenomenon that the solute-rich liquid between dendrites is washed out by the fluid motion of bulk liquid during solidification, the present investigation will show quantitatively the degree of washing against the transitional solidification layer which is composed of dendrites and the interdendritic liquid. The results will be applied to rimmed steel ingots.

II. Experimental Procedure

The method (1) of two concentric cylinders well-known as Taylor's vortex was used to change the flow velocity of bulk liquid on the basis of hydrodynamics. As the outer cylinder was at rest and the water-cooled inner cylinder was rotating, the solidification proceeded from the inner to the outer side. The specimen used was an Al–4wt%Cu alloy.

III. Experimental Results and the Analysis

Figure 1 shows the relation between the effective distribution coefficient, k^*, the rate of solidification, V, and the peripheral velocity, Us, of the solid/liquid interface moving with the inner cylinder in Al–4wt%Cu alloy. It might be considered that k^* was related to V. However, the detailed examination showed clearly that k^* depended on Us, as shown in Fig. 2. According to the Taylor's experiment,[2] the value of $U \times r$ is half the value of $Us \times r_0$, where U is the flow velocity, r_0 the radius of the inner cylinder and r the given radius from the center of the inner cylinder to the fluid. Therefore, the relation, $Us \approx 2U$, should be obtained in the vicinity of the solid/liquid interface. Thus k^* is expressed as follows:

$$U < 80\ \text{cm/sec}: \quad k^* = 1 - 6.86 \times 10^{-3} U \quad \text{......(1-a)}$$

$$U \geq 80\ \text{cm/sec}: \quad k^* = 0.45 \quad \text{......(1-b)}$$

IV. Theoretical Consideration on the Transitional Solidification Layer and the Effective Distribution Coefficient

1. *Transitional Solidification Layer*

The transitional solidification layer is divided into two layers, p and q on the basis of the authors' observation.[3] Both p and q layers are composed of solid and liquid. In the p layer the liquid is entrapped by the solid. Thus the solute concentration of the p layer remains unchanged after solidification. On the other hand, in the q layer the solids are existed within the liquid and solute-rich liquid can diffuse towards bulk liquid. Furthermore, the q layer is subdivided into q_1 and q_2 layers. In the q_1 layer the solid forms dendrite skeleton and the liquid can flow through the dendrite arm spacings. The q_2 layer belongs to the so-called pasty zone containing isolated solid particles.

Now let us consider the effective distribution coefficient of the transitional solidification layer, as shown

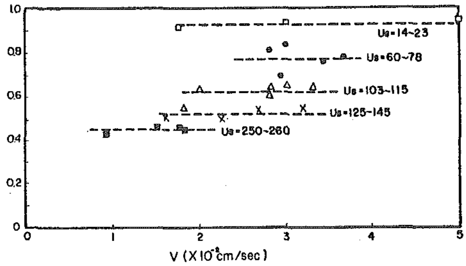

Fig. 1. Relation between effective distribution coefficient k^* and rate of solidification V for 5 levels of Us in Al–4 wt%Cu alloy (Us is peripheral velocity of the rotating solid surface)

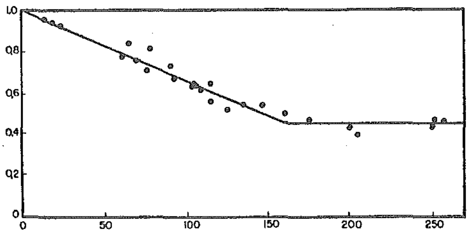

Fig. 2. Relation between effective distribution coefficient k^* and peripheral velocity of the rotating solid surface Us in Al–4 wt%Cu alloy

* Department of Metallurgical Engineering, Faculty of Engineering, Hokkaido University, Sapporo, Hokkaido 060, Japan.
** Department of Mechanical Engineering, Hokkaido Institute of Technology, Sapporo, Hokkaido 061–24, Japan.

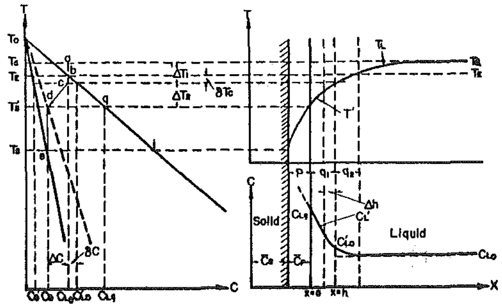

Fig. 3. Schematic representation of temperature and concentration distribution near the solid/liquid interface in binary alloys
T_0—i: liquidus line
T_0—d: virtual solidus line
T_0—e: solidus line

in Fig. 3. Using the equilibrium distribution coefficient, k_0, and the critical fraction of solid, Sp, above which q layer changes to p layer, the effective distribution coefficient is expressed as follows:

$$k^* = 1 - Sp(1-k_0) \quad \text{.....................(2)}$$

It is then necessary to determine the value of Sp when the solute-rich liquid between dendrites is completely washed out by the fluid motion of bulk liquid. Inserting $k_0=0.174$ and $k_m^*=0.45$, which is the minimum effective distribution coefficient of Eq. (1-b), into Eq. (2), Sp was calculated to be 67%.

2. Effective Distribution Coefficient

In order to obtain the effective distribution coefficient the mass balance and the temperature profile in the q layer were calculated theoretically.[1] Then, using the relation that the turbulent diffusivity is proportional to the turbulent flow velocity, U, and to the width, Δh, of the mixing zone,[1] the following equation is introduced:

$$1-k^* = \frac{B\Delta h\rho(Sp-\delta S)L}{aC_{L_0}K}\frac{U}{Z}(1-\delta S) \quad \text{.........(3)}$$

Where,

$$Z = \frac{\rho L(Sp-\delta S)/K}{\rho L\delta S/K + \Delta T_1/\alpha}$$

a: liquidus slope $(-dT/dC)$, K: thermal conductivity of the q layer, L: latent heat of fusion, ρ: density of the q layer, $\Delta T_1 = T_a - T_E + \delta T_c$ (see Fig. 3), T_a: tapping temperature, T_E: equilibrium liquidus temperature, δT_c: degree of undercooling, α: thermal diffusivity of bulk liquid and B: constant. δS is the fraction of solid which is formed initially at $x=h$ when undercooled by δT_c.

It is estimated that Δh and δS remain approximately constant in Eq. (3) except either in the initial and final stages of solidification, or in special conditions of slow cooling. Assuming that they are constant, all the factors but U in the right-hand side of Eq. (3) are constant. Then, the effective distribution coefficient is rewritten as follows:

$$k^* = 1 - EU \quad \text{.......................(4)}$$

where,
$$E = \frac{B\Delta h\rho(Sp-\delta S)L(1-\delta S)}{aC_{L_0}KZ}$$

According to the relation, k^* decreases linearly with increasing U. This agrees well with the experimental result of Eq. (1-a).

V. Application of the Experimental Results to Rimmed Steel Ingots

From the fact that the morphology and distribution of dendrites in steel are similar to those in Al–Cu alloy, the same critical fraction of solid as in Al–Cu alloy was adopted to determine the minimum effective distribution coefficients of C, Mn, P and S in the rimming ingots. They were obtained by substituting the fraction of solid of 67% and their equilibrium distribution coefficients into Eq. (2). However, some error must be considered in the determination of the minimum effective distribution coefficients, since several investigators have presented different values of the equilibrium distribution coefficients. Table 1 shows the calculated and observed values of the minimum effective distribution coefficients. It is recognized that these calculated values are approximately equal to the minimum effective distribution coefficients which have been observed in the rim-zone of rimming ingots.

VI. Conclusion

It was found that micro- and macro-segregation are controlled by the degree of washing against the transitional solidification layer with the fluid motion of bulk liquid.

REFERENCES

1) T. Takahashi and I. Hagiwara: *J. Jap. Inst. Metals*, **29** (1965), 1152.
2) G. I. Taylor: *Proc. Roy. Soc.*, A, **151** (1935), 494.
3) T. Takahashi and I. Hagiwara: *J. Jap. Inst. Metals*, **29** (1965), 631.
4) K. Guthmann: *Stahl u. Eisen*, **71** (1951), 399.
5) A. Hays and J. Chipman: *Trans. AIME*, **135** (1939), 85.
6) T. Wada: Preprints Abstract at the 61st Meeting of Japan Institute of Metals, October (1967), 174.
7) C. E. Sims: *Electric Furnace Steelmaking*, **2** (1963), 99, John Wiley & Sons, Inc.
8) W. A. Fisher, H. Spitzer, and M. Hishinura: *Arch. Eisenhüttenw.*, **31** (1960), 365.
9) R. L. Smith and J. L. Rutherford: *J. Metals*, **9** (1957), 478.
10) M. Hansen: Constitution of binary alloys, (1958), 705, McGraw-Hill Book Company, Inc.
11) S. Ishihara: *J. Iron Steel Inst. Japan*, **40** (1954), 403.
12) P. Nilles: *J. Iron Steel Inst.* (U.K.), **202** (1964), 601.
13) I. Kohira: Rimmed Steel Ingots, Reports of Technical Research Institute of Yawata Iron & Steel Works, Japan Iron & Steel Co. Ltd., Vol. 16, No. 1.
14) P. Bardenheuer and C. A. Müller: *K.-W.-Inst. Eisenforsch.*, **11** (1929), 225, 273.
15) A Stadeler and H. J. Tiele: *Stahl u. Eisen*, **31** (1931), 453.

Table 1. The minimum effective distribution coefficients in the rim-zone of rimming ingots

Alloying element	Equilibrium distribution coefficient			Minimum effective distribution coefficient		
	Phase	Value of k_0	Investigators	k^* (Calculated)	k^* (Observed)	Investigators
C	δ	0.13	K. Guthmann (4)	0.42	0.42	S. Ishihara (11)
			J. Chipman (5)		0.42	J. Chipman (5)
		0.17	T. Wada (6)	0.44	0.46	P. Nilles (12)
		0.20	C. E. Sims (7)	0.46	0.50	I. Kohira (13)
		0.29	W. A. Fisher (8)	0.52		
	γ	0.30	C. E. Sims (7)	0.53		
		0.34	T. Wada (6)	0.56		
		0.36	K. Guthmann (4)	0.57		
Mn	δ	0.76	T. Wada (6)	0.84	0.79 0.80 0.85 0.90 0.91	P. Bardenheuer (14)
		0.84	K. Guthmann (4)	0.89		
			J. Chipman (5)		0.90 0.91	I. Kohira (13)
		0.90	C. E. Sims (7)	0.93	0.90 0.92	J. Chipman (5)
	γ	0.75	C. E. Sims (7)	0.83	0.90 0.91 0.92	A. Stadeler (15)
		0.78	T. Wada (6)	0.85		
		0.95	K. Guthmann (4)	0.97	0.90	S. Ishihara (11)
P	δ	0.13	K. Guthmann (4)	0.42	0.38 0.46	P. Bardenheuer (14)
			J. Chipmann (5)			
		0.14	T. Wada (6)	0.42	0.63 0.65	T. Araki (16)
		0.2~0.5	R. E. Sims (9)	0.46~0.67		
	γ	0.06	K. Guthmann (4)	0.37		
		0.08	T. Wada (6)	0.38		
S	δ	0.02	K. Guthmann (4)	0.34	0.33 0.34 0.37	J. Matsuno (17)
			C. E. Sims (7)		0.36	Committee of I.S.I. (18)
		0.04	M. Hansen (10)	0.36	0.38 0.39 0.40 0.41 0.42	P. Bardenheuer (14)
		0.05	J. Chipman (5)	0.36		
		0.02	K. Guthmann (4)	0.34	0.41 0.42	I. Kohira (13)
		0.05	C. E. Sims (7)	0.36	0.41	S. Ishihara (11)

16) T. Araki and Y. Sugitani: *J. Iron Steel Inst.* Japan, **53** (1970), 106.

17) J. Matsuno: to be published.

18) Committee of the Iron and Steel Institute, 2nd Report: *J. Iron Steel Inst.*, **117** (1928), 401.

COMMENT

I. Golikov (Central Iron and Steel Research Institute, Moscow): The subject is phenomina of dendritic segregation in alloyed steels. Fe–Ni industrial ingots with additional elements such as: Al, W, Mo, B, C, Ti, Nb, Si, Sn were used. Next 5 main characteristics were determined:

(1) The degree of dendritic segregation development in hypoeutectic nickel-iron- and other elements base alloys is determined, under similar solidification conditions, with the type of alloying element. Elements, which form congruently melting compounds with the alloy base or one with another, have the segregation coefficient "K" perfectly higher than elements forming a solid solution or incongruent compounds.

(2) Components segregation direction and degree in complex alloys remains the same as in binary alloys, provided that alloy elements do not form congruently melting compounds.

(3) Elements that form congruent compounds essentially influence other components segregation in complex alloys, and this influence can be as strong as to cause the conversion of the segregation sign. Such elements in nickel-base alloys are: Ti, Ta, Nb, Sn, Si.

(4) Carbon has the strongest effect on its phenorence.

(5) Non-uniformity of distribution for the freely diffusing elements such as carbon, boron, nitrogen, is connected in the first line with their chemical interaction with the atoms of alloying additions.